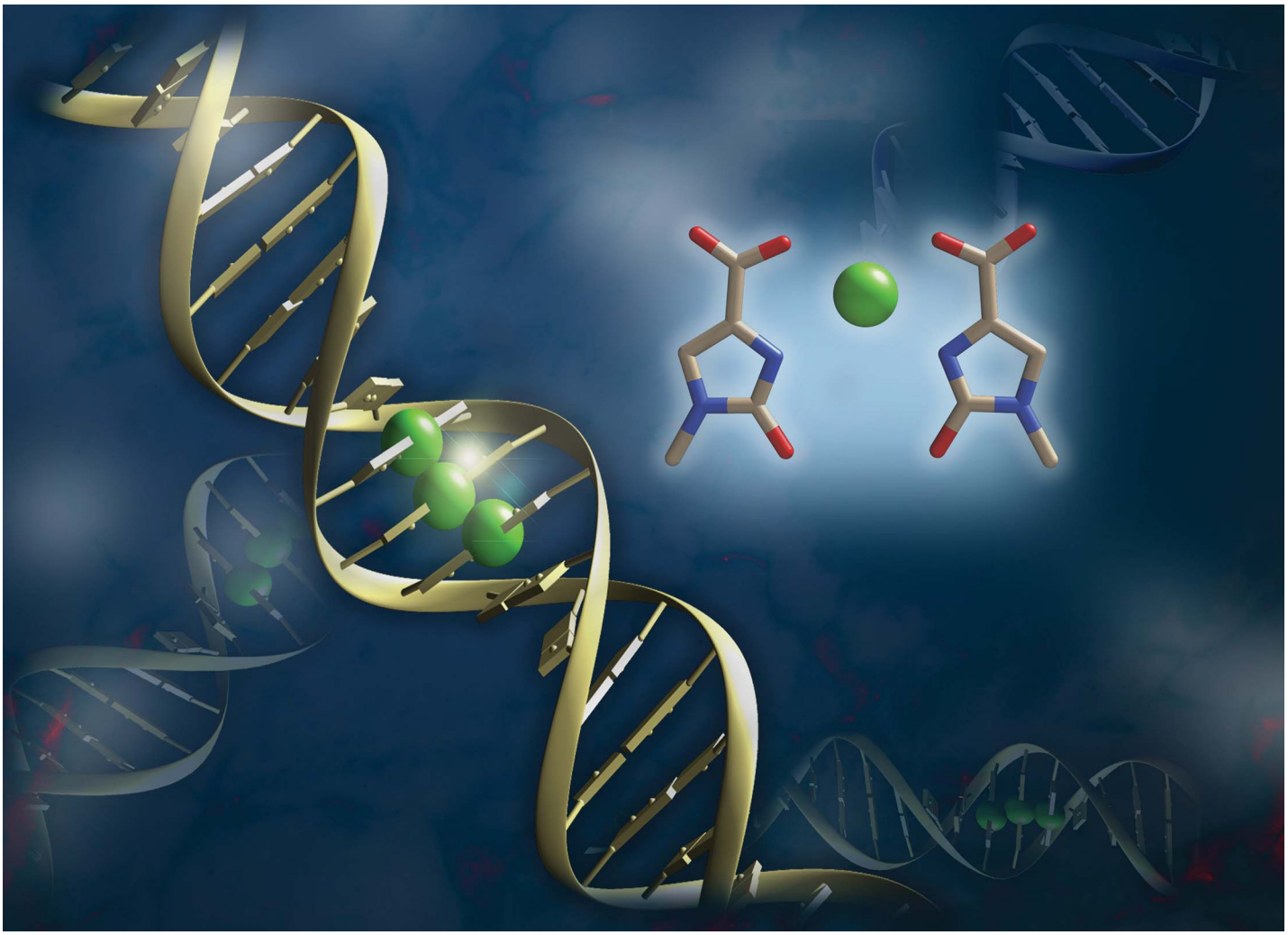

Showcasing research from Professor Shionoya's laboratory, Department of Chemistry, Graduate School of Science, the University of Tokyo, Tokyo, Japan.

Metal-mediated DNA base pairing of easily prepared 2-oxo-imidazole-4-carboxylate nucleotides

Metal-mediated DNA base pairing, consisting of two ligand-type artificial nucleobases and a bridging metal ion, has attracted increasing attention as an alternative base pairing mode to natural base pairing. In this study, we showed that a novel 2-oxo-imidazole-4-carboxylate (**Im**^{OC}) nucleobase, which can be easily derived from a commercially available uridine analogue, forms stable Cu^{II}- and Hg^{II}-mediated base pairs within DNA duplexes. Quantitative association of three Cu^{II} ions was also demonstrated in a duplex containing consecutive **Im**^{OC}–**Im**^{OC} pairs. This study will provide a new design strategy for metal-responsive DNA materials.

As featured in:

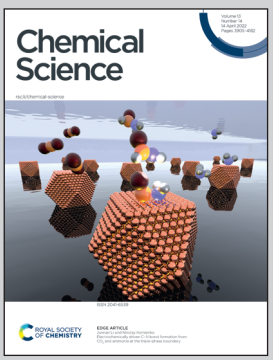

See Yusuke Takezawa, Mitsuhiko Shionoya *et al.*, *Chem. Sci.*, 2022, **13**, 3977.

ROYAL SOCIETY OF CHEMISTRY

rsc.li/chemical-science

Registered charity number: 207890

Chemical Science

ROYAL SOCIETY OF CHEMISTRY

EDGE ARTICLE

View Article Online
View Journal | View Issue

Cite this: *Chem. Sci.*, 2022, **13**, 3977

All publication charges for this article have been paid for by the Royal Society of Chemistry

Metal-mediated DNA base pairing of easily prepared 2-oxo-imidazole-4-carboxylate nucleotides†

Lingyun Hu, Yusuke Takezawa * and Mitsuhiko Shionoya *

Metal-mediated DNA base pairs, which consist of two ligand-type artificial nucleobases and a bridging metal ion, have attracted increasing attention in recent years as a different base pairing mode from natural base pairing. Metal-mediated base pairing has been extensively studied, not only for metal-dependent thermal stabilisation of duplexes, but also for metal assembly by DNA templates and construction of functional DNAs that can be controlled by metals. Here, we report the metal-mediated base paring properties of a novel 2-oxo-imidazole-4-carboxylate (Im^{OC}) nucleobase and a previously reported 2-oxo-imidazole-4-carboxamide (Im^{OA}) nucleobase, both of which can be easily derived from a commercially available uridine analogue. The Im^{OC} nucleobases were found to form stable Im^{OC}–Cu^{II}–Im^{OC} and Im^{OC}–Hg^{II}–Im^{OC} base pairs in the presence of the corresponding metal ions, leading to an increase in the duplex melting temperature by +20 °C and +11 °C, respectively. The Im^{OC} bases did not react with other divalent metal ions and showed superior metal selectivity compared to similar nucleobase design reported so far. The Im^{OC}–Cu^{II}–Im^{OC} base pair was much more stable than mismatch pairs with other natural nucleobases, confirming the base pair specificity in the presence of Cu^{II}. Furthermore, we demonstrated the quantitative assembly of three Cu^{II} ions inside a DNA duplex with three consecutive Im^{OC}–Im^{OC} pairs, showing great potential of DNA-template based Cu^{II} nanoarray construction. The study of easily-prepared Im^{OC} base pairs will provide a new design strategy for metal-responsive DNA materials.

Received 13th February 2022
Accepted 11th March 2022

DOI: 10.1039/d2sc00926a

rsc.li/chemical-science

Introduction

The high versatility and programming capabilities of DNA structures have served as a bridge from fundamental concepts to practicality in the field of DNA nanotechnology, which is a successful example of molecule-based bottom-up self-assembly processes.[1–6] Much attention has been focused on the construction of modified DNA monomers to further enrich the diversity of DNA structure and function.[7–9] In particular, a great deal of effort has been devoted to the development of artificial nucleobase pairs, which are increasingly being recognised as highly effective.[10,11] Among them, metal-mediated base pairing, which consists of two ligand-type artificial nucleobases and a bridging metal ion, has attracted increasing interest due to its unique coordination binding mode.[12–17] The newly introduced metal-mediated base pairs impart unique properties to the modified DNA, depending on the inherent nature of the metal. In addition to metal-dependent thermal stabilisation of duplexes, DNA-templated metal assembly,[18–23] modulation of charge transfer,[24–27] molecular sensing[28–30] and metal-dependent control of DNAzymes and aptamers[31–37] have been reported. Therefore, finding appropriate ligand-type nucleobases that can specifically and strongly bind to a certain metal ion and form metal-mediated base pairs is important to achieve these functions.

A variety of ligand-type artificial nucleobases have been developed so far by modifying simple ligand scaffolds such as pyridine,[38–40] maltol[41,42] and pyrimidine.[43–48] Among them, the imidazole ligand is one of the smallest scaffolds. It has been reported that most of the modified imidazole nucleobases form Ag^{I}-mediated base pairs by N–Ag^{I}–N coordination.[49–51] This metal binding property can be altered by introducing an additional coordination site.[52,53] For example, imidazole-4-carboxylate (Im^{C}) nucleobases form a base pair *via* Cu^{II}- and Ag^{I}-mediated coordination, and the negatively charged carboxylates neutralise the positive charge of the bridging metal ion.[52] The Im^{C}–Cu^{II}–Im^{C} pair is one of the most stabilising artificial base pairs developed so far,[35] but Im^{C} retains its binding affinity for other metals such as Ni^{II} and Co^{II}. Furthermore, we have successfully applied Im^{C}–Cu^{II}–Im^{C} pairing to the metal-dependent functional regulation of DNAzymes.[35]

Department of Chemistry, Graduate School of Science, The University of Tokyo, 7-3-1 Hongo, Bunkyo-ku, Tokyo 113-0033, Japan. E-mail: takezawa@chem.s.u-tokyo.ac.jp; shionoya@chem.s.u-tokyo.ac.jp

† Electronic supplementary information (ESI) available. See DOI: 10.1039/d2sc00926a

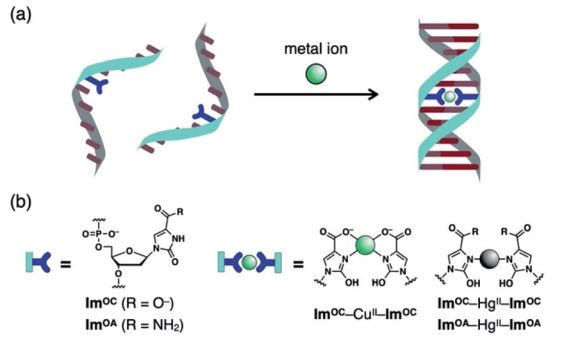

Fig. 1 (a) Schematic diagram of DNA duplexes with a metal-mediated base pair. (b) Molecular structures of novel ligand-type nucleotides bearing 2-oxo-imidazole-4-carboxylate (Im^{OC}) or 2-oxo-imidazole-4-carboxyamide (Im^{OA}) as a nucleobase. The expected structures of metal-mediated base pairs are also shown.

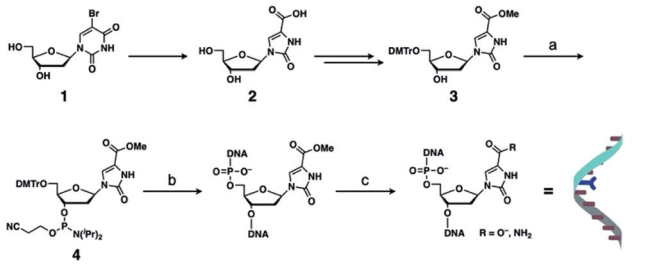

Scheme 1 Synthesis of DNA strands containing Im^{OC} or Im^{OA} nucleotides. The DMTr-modified nucleoside **3** was synthesised by the reported procedure.[55] (a) 2-Cyanoethyl *N*,*N*-diisopropylchlorophosphoramidite, DIPEA, CH_2Cl_2, rt, 0.5 h (78%); (b) DNA synthesiser; (c) 0.3 M NaOH aq., 37 °C (for Im^{OC}) or 25% ammonia aq., 55 °C (for Im^{OA}). DMTr = 4,4′-dimethoxytrityl.

With these examples as a starting point, we sought to expand the structural diversity of imidazole-like scaffolds that can form metal-mediated base pairs. Based on imidazole-4-carboxylate (Im^{C}), a novel ligand-type nucleobase, 2-oxo-imidazole-4-carboxylate (Im^{OC}), was designed by modifying the C-2 position (Fig. 1). Unlike conventional examples, Im^{OC} nucleosides can be easily derived from commercially available nucleosides,[54,55] reducing the need for laborious synthesis. The Im^{OC} nucleobase was predicted to have the following characteristics: (1) In contrast to the Im^{C} nucleobase, the N3 atom of Im^{OC} is protonated under neutral conditions.[56] Since metal coordination requires deprotonation or amide–iminol tautomerisation, Im^{OC} was expected to show a metal binding affinity different from the Im^{C} nucleobase. (2) As the Im^{C} nucleoside has a 2-carbonyl group, it preferentially adopts an *anti*-conformation suitable for metal-mediated base pairing, as reported for the 2-oxo-imidazole-4-carboxamide (Im^{OA}) nucleoside.[55] (3) The 2-carbonyl group may also function as a hydrogen bond acceptor for certain amino acids in DNA polymerases.[57,58] Therefore, such a structure may be advantageous for future polymerase incorporation studies.

In this study, DNA duplexes containing 2-oxo-imidazole-4-carboxylate (Im^{OC}) and 2-oxo-imidazole-4-carboxamide (Im^{OA}) were synthesised and their ability to form metal-mediated base pairs was investigated. Heterologous base pairing of Im^{OC} with other natural or unnatural nucleobases was also analysed in the presence and absence of certain metal ions. Furthermore, we investigated the construction of consecutive metal-mediated base pairs and explored the possibility of one-dimensional metal assembly inside DNA duplexes.

Results and discussion

Synthesis of DNA strands containing Im^{OC} or Im^{OA} nucleosides

The synthetic route for DNA strands containing Im^{OC} or Im^{OA} nucleosides is shown in Scheme 1. The 2-oxo-imidazole-4-carboxlate nucleoside (**2**) was synthesised by ring contraction of commercially available 5-bromo-2′-deoxyuridine (**1**).[54] Its protected derivative **3** was prepared by the reported procedure.[55] Phosphoramidite **4** was then synthesised without the N3 protection because the 3′-NH group was found to be intact during DNA synthesis just like thymidine. The resulting phosphoramidite was immediately used for solid-phase DNA synthesis.

Since the 4′-substituent was protected as a methyl ester, the nucleobase moiety can be converted to either a carboxylate (Im^{OC}) or a carboxamide (Im^{OA}) depending on the deprotection conditions. To confirm this, we synthesised a trimer DNA strand with one unnatural nucleotide (5′-**TXT**-3′) and deprotected it with sodium hydroxide or ammonia solution. The deprotected products were analysed by HPLC (Fig. S1†) and ESI mass spectrometry (Fig. S2†). When the trinucleotide was treated with 0.3 M NaOH aq. at 37 °C, an almost complete conversion to the carboxylate Im^{OC} was observed. When incubated in 25% ammonia solution, the artificial nucleobase was converted to the desired amide Im^{OA} in over 90% yield. The strands containing Im^{OC} and Im^{OA} were easily isolated by reverse-phase HPLC.

To investigate the metal-mediated base-pairing properties of Im^{OC} and Im^{OA} nucleotides, 15-mer DNA strands containing one or three Im^{OC}/Im^{OA} nucleotides in the central position were synthesised (Table 1). All the strands were deprotected with NaOH or ammonia solution to produce Im^{OC} or Im^{OA} nucleobases, which were purified by HPLC (Fig. S3†). The DNA

Table 1 Sequences of DNA strands used in this study

DNA	Sequences (5′ to 3′)[a]
1	CAC ATT AIm^{OC}T GTT GTA
2	TAC AAC AIm^{OC}T AAT GTG
2N (N = A, T, G, C)	TAC AAC ANT AAT GTG
3	CAC ATT AIm^{OA}T GTT GTA
4	TAC AAC AIm^{OA}T AAT GTG
5	CAC ATT $Im^{OC}Im^{OC}Im^{OC}$ GTT GTA
6	TAC AAC $Im^{OC}Im^{OC}Im^{OC}$ AAT GTG
7	CAC ATT AIm^{C}T GTT GTA
8	TAC AAC AIm^{C}T AAT GTG

[a] Im^{C}: imidazole-4-carboxylate.

oligomers with the desired artificial nucleotides were characterised by ESI mass spectrometry (see ESI†).

Cu^{II}-mediated base pairing of Im^{OC} nucleobases

Metal-mediated base pairing was first examined in a duplex containing a single artificial base pair, $\mathbf{Im^{OC}}$–$\mathbf{Im^{OC}}$ or $\mathbf{Im^{OA}}$–$\mathbf{Im^{OA}}$. Thermal melting analysis of duplexes **1·2** and **3·4** was performed in the absence and presence of various metal ions (1.0 equiv.), including first-row transition metal ions and square-planar Pd^{II} and Pt^{II} ions (Fig. 2, S4, and Table S1†). In the absence of metal ions, the melting temperatures (T_m) of the $\mathbf{Im^{OC}}$-modified duplex **1·2** and $\mathbf{Im^{OA}}$-modified duplex **3·4** were 23.0 °C and 34.5 °C, respectively. Both duplexes were significantly less stable than a fully matched duplex containing an A–T pair in the middle (T_m = 44.2 °C),[33] indicating that both $\mathbf{Im^{OC}}$–$\mathbf{Im^{OC}}$ and $\mathbf{Im^{OA}}$–$\mathbf{Im^{OA}}$ behave as mismatch pairs. The T_m value of duplex **1·2** is about 12 °C lower than that of duplex **3·4**. This may be due to the coulombic repulsion between the negatively charged carboxylates of the $\mathbf{Im^{OC}}$–$\mathbf{Im^{OC}}$ base pair. A similar phenomenon was also observed in the DNA duplex containing a pair of imidazole-4-carboxylate nucleobases ($\mathbf{Im^{C}}$), which showed a T_m value (22.5 °C) similar to that of the $\mathbf{Im^{OC}}$-containing duplex **1·2**.[35] Among the metal ions tested, only the Cu^{II} ion showed significant stabilisation of duplex **1·2** (T_m = 43.3 °C, ΔT_m = +20.3 °C). On the other hand, none of these metal ions caused a significant change in the melting profile of duplex **3·4** (-1 °C ≤ ΔT_m ≤ +1 °C). The Cu^{II}-dependent stabilisation of duplex **1·2** suggests the Cu^{II}-mediated formation of the $\mathbf{Im^{OC}}$–Cu^{II}–$\mathbf{Im^{OC}}$ base pair, which crosslinks the duplex *via* metal coordination bonds.

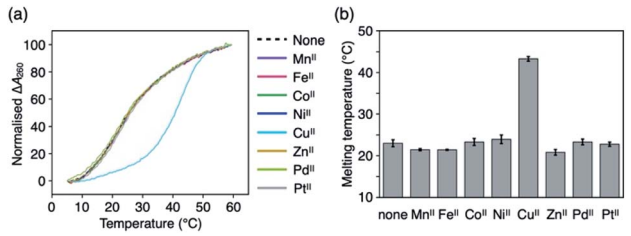

Fig. 2 (a) Melting curves of a DNA duplex containing an $\mathbf{Im^{OC}}$–$\mathbf{Im^{OC}}$ base pair (**1·2**) in the presence of various metal ions. [duplex] = 2.0 μM, [metal ion]/[duplex] = 0 (dashed line) or 1 (solid lines) in 10 mM HEPES buffer (pH 7.0), 100 mM NaCl, 0.2 °C min^{-1}. (b) Melting temperatures. N = 3. The error bars represent the standard errors.

Fig. 3a shows the melting curves of duplex **1·2** in the presence of various amounts of Cu^{II} ions. In the presence of 0.5 equiv. of Cu^{II} ions, a two-step transition was observed, indicating the presence of both metal-free and Cu^{II}-bound DNA duplexes. The addition of more than one equivalent of Cu^{II} did not cause any obvious change in the melting behaviour. In addition, Cu^{II}-dependent stabilisation was not observed in the fully matched duplex or in the duplex containing a T–T mismatch.[33,41] These results proved that the metal-mediated base pair was formed by the binding of a single Cu^{II} ion, and also indicated that there is a high binding affinity between $\mathbf{Im^{OC}}$ and Cu^{II}. The stoichiometry of the $\mathbf{Im^{OC}}$–Cu^{II}–$\mathbf{Im^{OC}}$ base pair was further confirmed by ESI-TOF mass spectrometry (found: 1838.41 (z = 5); calcd. for $[\mathbf{1\cdot2} + Cu^{II} - 7H]^{5-}$: 1838.47; Fig. 3b and S5†).

It is suggested that the $\mathbf{Im^{OC}}$–Cu^{II}–$\mathbf{Im^{OC}}$ pair is formed by the coordination of both the N3 atoms and the carboxylate groups in a square planar geometry. Cu^{II}-mediated base pairing with similar coordination structures has been reported with imidazole-4-carboxylate nucleobases ($\mathbf{Im^{C}}$)[52] and with 6-carboxypurines.[59] The carboxylate group of the $\mathbf{Im^{OC}}$ nucleobases not only coordinates with the Cu^{II} ion, but also neutralises the positive charge of the metal, thus maintaining a neutral environment within the DNA duplex. However, in the case of the $\mathbf{Im^{OA}}$ nucleobase, the carboxamide group is a weak neutral ligand and cannot neutralise the resulting complex. This is the main reason why metal-mediated base pairing with $\mathbf{Im^{OA}}$ is unfavourable.

The circular dichroism (CD) spectra of duplex **1·2** were also measured in the absence and presence of Cu^{II} ions (Fig. 3c). The spectra showed Cotton effects characteristic of right-handed B-DNA, indicating that the introduction of the $\mathbf{Im^{OC}}$–Cu^{II}–$\mathbf{Im^{OC}}$ base pair did not alter the typical duplex structure. Due to the small size of the $\mathbf{Im^{OC}}$ base, the π–π stacking interaction with the neighbouring base pairs may be reduced, making the

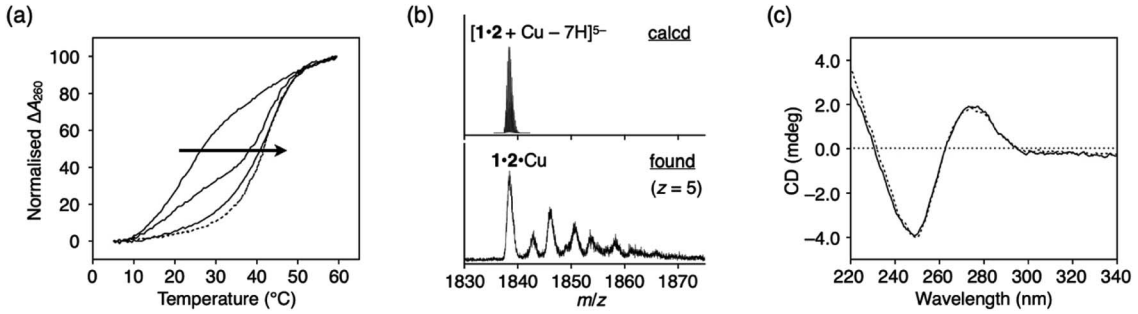

Fig. 3 (a) Melting curves of the DNA duplex **1·2** containing an $\mathbf{Im^{OC}}$–$\mathbf{Im^{OC}}$ base pair in the presence of different concentrations of Cu^{II} ions. [duplex] = 2.0 μM, [Cu^{II}]/[duplex] = 0, 0.5, 1 (solid lines), 2, and 3 (dashed lines) in 10 mM HEPES buffer (pH 7.0), 100 mM NaCl, 0.2 °C min^{-1} (b) ESI mass spectrum of the duplex **1·2** with 1 equiv. of Cu^{II} (negative mode). Small signals were attributed to the sodium and potassium adducts. See also Fig. S5.† (c) CD spectra of the duplex **1·2** in the absence (dotted lines) and presence (solid lines) of 1 equiv. of Cu^{II}. [duplex] = 2.0 μM in 10 mM HEPES buffer (pH 7.0), 100 mM NaCl, l = 0.5 cm, 4 °C.

duplex less stable. However, this destabilisation effect can be compensated for by the coordination bonds of $\mathbf{Im^{OC}}$–Cu^{II}–$\mathbf{Im^{OC}}$. Overall, the stability of the duplex containing an $\mathbf{Im^{OC}}$–Cu^{II}–$\mathbf{Im^{OC}}$ pair ($\mathbf{1\cdot2}\cdot Cu^{II}$, T_m = 43.3 °C) was completely comparable to that of the natural DNA duplex (44.2 °C).

It should be emphasised that $\mathbf{Im^{OC}}$ showed better metal selectivity for Cu^{II} compared to the structurally relevant imidazole-4-carboxylate ($\mathbf{Im^{C}}$) nucleobase.[35,52] A DNA duplex with an $\mathbf{Im^{C}}$–$\mathbf{Im^{C}}$ base pair was stabilised by the addition of not only Cu^{II} (ΔT_m = +35.2 °C) but also many transition metal ions such as Ni^{II} and Co^{II} (+14.0 °C and + 11.3 °C, respectively).[35] In contrast to $\mathbf{Im^{C}}$, the N3 atom of $\mathbf{Im^{OC}}$ needs to be deprotonated for metal complexation. Thus, $\mathbf{Im^{OC}}$ showed excellent metal selectivity in that it forms metal-mediated base pairs with only the most suitable Cu^{II}.

Hg^{II}-mediated base pairing of Im^{OC}/Im^{OA} nucleobases

Hg^{II} and Ag^{I} ions are often involved in metal-mediated base pairing in two-coordinate geometry, such as the classical T–Hg^{II}–T[60,61] and C–Ag^{I}–C[62] base pairs. Since the 2-oxo-imidazole ring is derived from uridine/thymine nucleobases, $\mathbf{Im^{OC}}$ and $\mathbf{Im^{OA}}$ were expected to form a metal-mediated base pair similar to T–Hg^{II}–T. To investigate this, we conducted melting analysis of duplexes $\mathbf{1\cdot2}$ and $\mathbf{3\cdot4}$ in the presence of Hg^{II} or Ag^{I} ions (Fig. 4, S6 and Table S2†). In these measurements, sodium chloride in the buffer solution was replaced by sodium nitrate to prevent precipitation of metal chlorides.

The addition of one equivalent of Hg^{II} ions markedly increased the stability of both $\mathbf{Im^{OC}}$- and $\mathbf{Im^{OA}}$-containing duplexes (ΔT_m = +11.4 °C and +6.2 °C for duplexes $\mathbf{1\cdot2}$ and $\mathbf{3\cdot4}$, respectively). The addition of excess Hg^{II} did not stabilise the duplexes anymore (Fig. S7†). This suggests that the formation of $\mathbf{Im^{OC}}$–Hg^{II}–$\mathbf{Im^{OC}}$ and $\mathbf{Im^{OA}}$–Hg^{II}–$\mathbf{Im^{OA}}$ base pairs is mediated by a single Hg^{II} ion. The Hg^{II}-mediated base pairing was further confirmed by ESI-MS measurements of the $\mathbf{Im^{OC}}$-containing duplex (found: 2342.26 (z = 4); calcd for $[\mathbf{1\cdot2} + Hg^{II} + K^{I} - 7H]^{4-}$: 2342.11; Fig. S8†) and the $\mathbf{Im^{OA}}$-containing one (found: 2332.08 (z = 4); calcd. for $[\mathbf{3\cdot4} + Hg^{II} - 6H]^{4-}$: 2332.13; Fig. S9†). $\mathbf{Im^{OC}}$ and $\mathbf{Im^{OA}}$ are thought to form a linear complex with Hg^{II} *via* coordination of the deprotonated N3 atom, similar to the T–Hg^{II}–T base pair.[63,64] It is noteworthy that in the case of $\mathbf{Im^{OC}}$, the degree of Hg^{II}-dependent duplex stabilisation is comparable to that observed for the T–Hg^{II}–T base pair (ΔT_m = +10.9 °C) under the same conditions.[33]

Notably, the addition of Ag^{I} did not stabilise the duplexes containing $\mathbf{Im^{OC}}$ and $\mathbf{Im^{OA}}$. On the other hand, previous studies have shown that the duplex with an imidazole-4-carboxylate base pair ($\mathbf{Im^{C}}$–$\mathbf{Im^{C}}$) is stabilised by both Hg^{II} and Ag^{I} ions, with a slightly higher preference for Ag^{I} over Hg^{II}.[35,52] These results indicate that $\mathbf{Im^{OC}}$ and $\mathbf{Im^{OA}}$ nucleobases improve the metal selectivity, which can be attributed to the protonated N3 atoms. Therefore, $\mathbf{Im^{OC}}$ and $\mathbf{Im^{OA}}$ bases are more suitable for the construction of complex molecular systems using multiple types of metal ions.

Heterologous base pairing of Im^{OC} with other natural and unnatural nucleobases

Apart from the homologous base pairing, base pairing between $\mathbf{Im^{OC}}$ and other nucleobases was also examined to clarify the specificity. First, mismatch base pairing with four natural nucleobases was evaluated by duplex melting analysis (Fig. 5a and Table S3†). The T_m values of the duplexes with an $\mathbf{Im^{OC}}$–N pair (N = A, T, C and G) were different, and the pyrimidine mismatches ($\mathbf{Im^{OC}}$–T and $\mathbf{Im^{OC}}$–C) were found to be less stable than the purine mismatches ($\mathbf{Im^{OC}}$–A and $\mathbf{Im^{OC}}$–G). This trend can be well explained by the fact that the size of the $\mathbf{Im^{OC}}$–purine pairs is comparable to that of the natural base pairs. Similar results were also obtained in previous studies examining $\mathbf{Im^{OA}}$–N base pairing.[55] The addition of one equivalent of Cu^{II} ions did not cause an obvious T_m change, indicating that $\mathbf{Im^{OC}}$ does not form Cu^{II}-mediated base pairs with natural nucleobases. It is important to note that the T_m value of the duplex containing $\mathbf{Im^{OC}}$–Cu^{II}–$\mathbf{Im^{OC}}$ is higher than all other duplexes with an $\mathbf{Im^{OC}}$–N pair. This result shows the specificity of the $\mathbf{Im^{OC}}$–Cu^{II}–$\mathbf{Im^{OC}}$ base pairing over pairing with natural nucleobases in the presence of Cu^{II} ions.

Next, we investigated the possibility of heterologous base pairing between $\mathbf{Im^{C}}$ and $\mathbf{Im^{OC}}$ in relation to the previously studied $\mathbf{Im^{C}}$–Cu^{II}–$\mathbf{Im^{C}}$ base pair (Fig. 5b, S10 and Table S4†). As expected, the duplex melting analysis showed that the $\mathbf{Im^{OC}}$–

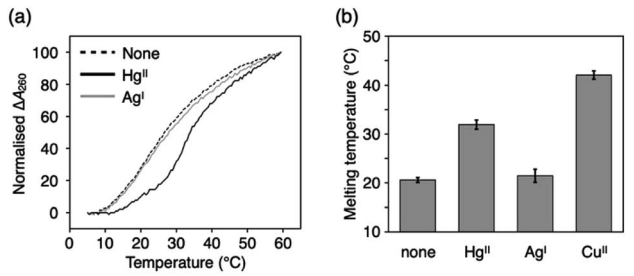

Fig. 4 (a) Melting curves of a DNA duplex containing an Im^{OC}–Im^{OC} base pair (**1·2**) in the presence of Hg^{II} and Ag^{I} ions. [duplex] = 2.0 μM, [metal ion]/[duplex] = 0 (dashed line) or 1 (solid lines) in 10 mM HEPES buffer (pH 7.0), 100 mM $NaNO_3$, 0.2 °C min^{-1}. (b) Melting temperatures. N = 3. The error bars represent the standard errors. The melting temperature in the same buffer in the presence of Cu^{II} is also shown.

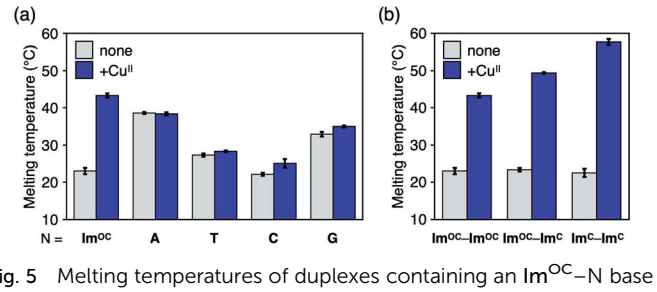

Fig. 5 Melting temperatures of duplexes containing an Im^{OC}–N base pair (**1·2N**; N = A, T, C, G) in the absence and presence of 1 equiv. of Cu^{II}. (b) Melting temperatures of duplexes containing an Im^{OC}–Im^{OC} (**1·2**), an Im^{OC}–Im^{C} (**1·8**), or an Im^{C}–Im^{C} base pair (**7·8**) in the absence and presence of 1 equiv. of Cu^{II}. [duplex] = 2.0 μM and [Cu^{II}]/[duplex] = 0 or 1 in 10 mM HEPES buffer (pH 7.0) and 100 mM NaCl. N = 3. The error bars represent the standard errors.

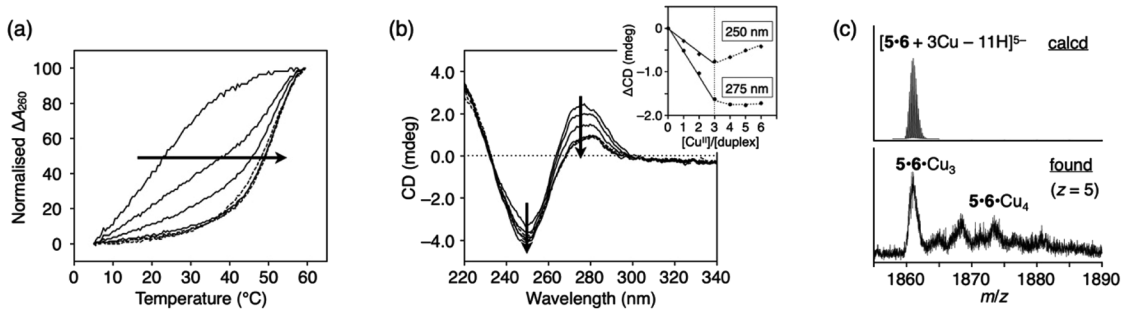

Fig. 6 (a) Melting curves of DNA duplex **5·6** containing three Im^{OC}–Im^{OC} base pairs in the presence of different concentrations of Cu^{II} ions. [duplex] = 2.0 μM, [Cu^{II}]/[duplex] = 0, 1, 2, 3 (solid lines), and 4, 5, and 6 (dashed lines). (b) CD spectra of duplex **5·6** in the presence of different concentrations of Cu^{II} ions. [Cu^{II}]/[duplex] = 0, 1, 2, 3 (solid lines) and 4, 5, and 6 (dotted lines). The changes in intensity at 250 and 275 nm are plotted in the inset. (c) ESI mass spectrum of duplex **5·6** with 3 equiv. of Cu^{II} (negative mode). See also Fig. S11.† The conditions are the same as in Fig. 3.

Cu^{II}–$\mathbf{Im^C}$ heterologous base pair was formed in the presence of Cu^{II} ions (ΔT_m = +26.1 °C). The ΔT_m value was intermediate between those of the duplexes containing the $\mathbf{Im^{OC}}$–Cu^{II}–$\mathbf{Im^{OC}}$ and $\mathbf{Im^C}$–Cu^{II}–$\mathbf{Im^C}$ pairs. This result reflects the Cu^{II} binding affinity of $\mathbf{Im^{OC}}$ and $\mathbf{Im^C}$ described above.

DNA-templated metal assembly using Im^{OC} nucleobases

The construction of one-dimensional metal arrays using DNA as a template is one of the promising applications of metal-mediated base pairing.[18–23] To investigate the possibility of DNA-templated metal assembly using $\mathbf{Im^{OC}}$ nucleobases, a 15-mer duplex with three consecutive $\mathbf{Im^{OC}}$–$\mathbf{Im^{OC}}$ base pairs in the centre (duplex **5·6**) was prepared.

Duplex melting experiments were conducted in the presence of different amounts of Cu^{II} ions (Fig. 6a). In the absence of Cu^{II} ions, duplex **5·6** was highly unstable, and the T_m value could not be determined. As the amount of Cu^{II} ions increased, the melting curves gradually shifted. When 3 equiv. of Cu^{II} ions were added, the T_m value was almost at its maximum (T_m = 51.7 °C). The melting curves were hardly changed by the addition of excess Cu^{II}. These results show that three base pairs of $\mathbf{Im^{OC}}$–Cu^{II}–$\mathbf{Im^{OC}}$ were quantitatively formed in duplex **5·6**. The T_m value of duplex **5·6** with 3 equiv. of Cu^{II} is about 10 °C higher than that of duplex **1·2** with equimolar Cu^{II}. This indicates that the incorporation of multiple $\mathbf{Im^{OC}}$–Cu^{II}–$\mathbf{Im^{OC}}$ base pairs enhances the duplex stability more efficiently.

The stoichiometric formation of the $\mathbf{Im^{OC}}$–Cu^{II}–$\mathbf{Im^{OC}}$ base pairs was further examined by circular dichroism (CD) measurements at 4 °C (Fig. 6b). In contrast to the CD spectra of duplexes **1·2** and **3·4**, the CD spectrum of duplex **5·6** showed a dramatic change upon Cu^{II} addition. As the amount of Cu^{II} ions increased, the CD intensity at 275 nm gradually decreased. The spectra changed linearly in the range of [Cu^{II}]/[**5·6**] = 0 to 3 and did not change with the addition of more than 3 equiv. of Cu^{II}. The result of the CD measurements were in excellent agreement with the behaviours of the melting curves, indicating that three Cu^{II} ions were bound within duplex **5·6**. Such stoichiometry was also confirmed by ESI-MS measurements, where a duplex containing three Cu^{II} ions was mainly observed (found: 1860.92 (z = 5); calcd. for [**5·6** + 3Cu^{II} − 11H]$^{5-}$: 1860.84; Fig. 6c and S11†). These results suggest that the three Cu^{II} ions were quantitatively assembled inside the duplex due to the formation of the $\mathbf{Im^{OC}}$–Cu^{II}–$\mathbf{Im^{OC}}$ base pairs. Thus, it was shown that a certain number of Cu^{II} ions can be aligned according to the number of $\mathbf{Im^{OC}}$ bases in the template DNA duplex.

Conclusions

In this study, we have shown that a novel 2-oxo-imidazole-4-carboxylate ($\mathbf{Im^{OC}}$) nucleobase undergoes metal-mediated base pairing in DNA duplexes. The previously reported synthetic route for the corresponding phosphoramidite[55] was shortened by removing one unnecessary protection step. The protected artificial nucleobase(s) in DNA oligomers can be easily converted to two types of nucleobases, $\mathbf{Im^{OC}}$ and the previously reported carboxamide ($\mathbf{Im^{OA}}$), depending on the deprotection conditions. Other than the natural T and C bases, $\mathbf{Im^{OC}}$ and $\mathbf{Im^{OA}}$ are among the most easily prepared nucleobases that can form metal-mediated base pairs.

The metal-mediated base pairing of both nucleobases was studied by duplex melting analysis, CD spectrometry and mass spectrometry. It was found that the $\mathbf{Im^{OC}}$ homologous base pair forms stable metal-mediated base pairs with both Cu^{II} and Hg^{II} (*i.e.*, $\mathbf{Im^{OC}}$–Cu^{II}–$\mathbf{Im^{OC}}$ and $\mathbf{Im^{OC}}$–Hg^{II}–$\mathbf{Im^{OC}}$), and ΔT_m was +20.0 °C and +11.4 °C, respectively. In contrast, $\mathbf{Im^{OA}}$ showed only a slight increase in T_m in the presence of Hg^{II} (ΔT_m = +6.2 °C) due to the formation of the $\mathbf{Im^{OA}}$–Hg^{II}–$\mathbf{Im^{OA}}$ pair. This difference in metal ion affinity is mainly due to the substituent at the 4-position, since the negative carboxylate group can form a stronger coordination bond with Cu^{II}. Probably due to the protonated N3 atom, $\mathbf{Im^{OC}}$ was found to exhibit superior metal selectivity compared to the structurally related imidazole-4-carboxylate ($\mathbf{Im^C}$) nucleobase.[35,52]

Further investigation of the possibility of heterologous base pairing in the absence and presence of metal ions revealed that the $\mathbf{Im^{OC}}$–Cu^{II}–$\mathbf{Im^{OC}}$ base pair was more stable than heterologous base pairing with natural nucleobases (*i.e.* $\mathbf{Im^{OC}}$–N), suggesting the specificity of metal-mediated homologous base pairing among the possible base pairing patterns. When paired with the previously reported $\mathbf{Im^C}$, the resulting $\mathbf{Im^{OC}}$–Cu^{II}–$\mathbf{Im^C}$

heterologous base pair showed intermediate stability (ΔT_m = +26.1 °C) between $\mathbf{Im^{OC}}$–Cu^{II}–$\mathbf{Im^{OC}}$ (+20.3 °C) and $\mathbf{Im^{C}}$–Cu^{II}–$\mathbf{Im^{C}}$ (+35.2 °C). This result indicates that the metal-mediated base pair stabilisation effect can be rationally tuned by replacing the ligand-type nucleobases.

The stable $\mathbf{Im^{OC}}$–Cu^{II}–$\mathbf{Im^{OC}}$ base pairing is expected to have applications such as the construction of DNA-templated metal arrays. In the preliminary experiments using a duplex containing three $\mathbf{Im^{OC}}$–$\mathbf{Im^{OC}}$ base pairs, we succeeded in quantitatively assembling three Cu^{II} ions. Since the $\mathbf{Im^{OC}}$ nucleoside can be prepared from a commercially available nucleoside by a short-step synthesis, $\mathbf{Im^{OC}}$ oligomers are considered suitable for constructing one dimensional metal wires. In addition, the significant increase in duplex stability and high metal selectivity brought by the formation of the $\mathbf{Im^{OC}}$–Cu^{II}–$\mathbf{Im^{OC}}$ base pair makes it a promising candidate for constructing metal-responsive DNA nanodevices and nanomachines. The newly introduced 2-oxo functional group is expected to play an important role in recognition by DNA polymerases. Applications such as enzymatic synthesis[65,66] and PCR amplification[67] are highly promising and will be probed in the future. Thus, metal-mediated base pairing with $\mathbf{Im^{OC}}$ is believed to have high potential applications in DNA supramolecular chemistry and nanotechnology.

Data availability

All the data are shown in the ESI.†

Author contributions

Y. T. and M. S. conceived and directed the study. L. H. performed the experiments and analysed the data with the aid of Y. T. All the authors prepared the manuscript.

Conflicts of interest

There are no conflicts to declare.

Acknowledgements

This work was supported by JSPS KAKENHI grant numbers JP18H02081, JP21H02055, JP21H00384 (Molecular Engine) and JP21H05866 (Molecular Cybernetics) (to Y. T.), JP16H06509 (Coordination Asymmetry) and JP21H05022 (to M. S.) and JP21J11332 (Grant-in-Aid for JSPS Fellows; to L. H.). Y. T. also acknowledges financial support from the Iketani Science and Technology Foundation.

Notes and references

1 N. C. Seeman and H. F. Sleiman, *Nat. Rev. Mater.*, 2017, **3**, 17068–17091.
2 M. Madsen and K. V. Gothelf, *Chem. Rev.*, 2019, **119**, 6384–6458.
3 P. Chidchob and H. F. Sleiman, *Curr. Opin. Chem. Biol.*, 2018, **46**, 63–70.
4 S. Nummelin, B. X. Shen, P. Piskunen, Q. Liu, M. A. Kostiainen and V. Linko, *ACS Synth. Biol.*, 2020, **9**, 1923–1940.
5 Y. G. Ke, C. Castro and J. H. Choi, *Annu. Rev. Biomed. Eng.*, 2018, **20**, 375–401.
6 E. Stulz and G. H. Clever, *DNA in supramolecular chemistry and nanotechnology*, Wiley, Chichester, 2015.
7 K. Nakatani and Y. Tor, *Modified Nucleic Acids*, Springer, 2016.
8 L. K. McKenzie, R. El-Khoury, J. D. Thorpe, M. J. Damha and M. Hollenstein, *Chem. Soc. Rev.*, 2021, **50**, 5126–5164.
9 V. B. Pinheiro and P. Holliger, *Trends Biotechnol.*, 2014, **32**, 321–328.
10 A. W. Feldman and F. E. Romesberg, *Acc. Chem. Res.*, 2018, **51**, 394–403.
11 M. Kimoto and I. Hirao, *Chem. Soc. Rev.*, 2020, **49**, 7602–7626.
12 Y. Takezawa and M. Shionoya, *Acc. Chem. Res.*, 2012, **45**, 2066–2076.
13 Y. Takezawa, J. Müller and M. Shionoya, *Chem. Lett.*, 2017, **46**, 622–633.
14 Y. Takezawa, M. Shionoya and J. Müller, in *Comprehensive Supramolecular Chemistry II*, ed. J. L. Atwood, Elsevier, Oxford, 2017, vol. 4, pp. 259–293.
15 S. Naskar, R. Guha and J. Müller, *Angew. Chem., Int. Ed.*, 2020, **59**, 1397–1406.
16 J. Müller, *Coord. Chem. Rev.*, 2019, **393**, 37–47.
17 D. Ukale and T. Lönnberg, *ChemBioChem*, 2021, **22**, 1733–1739.
18 K. Tanaka, A. Tengeiji, T. Kato, N. Toyama and M. Shionoya, *Science*, 2003, **299**, 1212–1213.
19 K. Tanaka, G. H. Clever, Y. Takezawa, Y. Yamada, C. Kaul, M. Shionoya and T. Carell, *Nat. Nanotechnol.*, 2006, **1**, 190–194.
20 Y. Takezawa, W. Maeda, K. Tanaka and M. Shionoya, *Angew. Chem., Int. Ed.*, 2009, **48**, 1081–1084.
21 G. H. Clever and T. Carell, *Angew. Chem., Int. Ed.*, 2007, **46**, 250–253.
22 J. Kondo, Y. Tada, T. Dairaku, Y. Hattori, H. Saneyoshi, A. Ono and Y. Tanaka, *Nat. Chem.*, 2017, **9**, 956–960.
23 Y. Takezawa and M. Shionoya, in *Biomimetics Bioinspired Materials, Mechanics, and Dynamics, Handbook of Biomimetics and Bioinspiration*, ed. E. Jabbari, D.-H. Kim, L. P. Lee, A. Ghaemmaghami and A. Khademhosseini, World Scientific Publishing, Singapore, 2014, vol. 1, pp. 217–245.
24 S. Liu, G. H. Clever, Y. Takezawa, M. Kaneko, K. Tanaka, X. Guo and M. Shionoya, *Angew. Chem., Int. Ed.*, 2011, **50**, 8886–8890.
25 J. Joseph and G. B. Schuster, *Org. Lett.*, 2007, **9**, 1843–1846.
26 T. Ehrenschwender, W. Schmucker, C. Wellner, T. Augenstein, P. Carl, J. Harmer, F. Breher and H.-A. Wagenknecht, *Chem.–Eur. J.*, 2013, **19**, 12547–12552.
27 S. Hensel, K. Eckey, P. Scharf, N. Megger, U. Karst and J. Müller, *Chem.–Eur. J.*, 2017, **23**, 10244–10248.
28 A. Ono and H. Togashi, *Angew. Chem., Int. Ed.*, 2004, **43**, 4300–4302.

29 B. Jash and J. Müller, *Eur. J. Inorg. Chem.*, 2017, **33**, 3857–3861.
30 S. Taherpour, O. Golubev and T. Lönnberg, *Inorg. Chim. Acta*, 2016, **452**, 43–49.
31 J. Liu and Y. Lu, *Angew. Chem., Int. Ed.*, 2007, **46**, 7587–7590.
32 S. Shimron, J. Elbaz, A. Henning and I. Willner, *Chem. Commun.*, 2010, **46**, 3250–3252.
33 Y. Takezawa, T. Nakama and M. Shionoya, *J. Am. Chem. Soc.*, 2019, **141**, 19342–19350.
34 T. Nakama, Y. Takezawa, D. Sasaki and M. Shionoya, *J. Am. Chem. Soc.*, 2020, **142**, 10153–10162.
35 Y. Takezawa, L. Hu, T. Nakama and M. Shionoya, *Angew. Chem., Int. Ed.*, 2020, **59**, 21488–21492.
36 M. H. Heddinga and J. Müller, *Beilstein J. Org. Chem.*, 2020, **16**, 2870–2879.
37 T. Nakama, Y. Takezawa and M. Shionoya, *Chem. Commun.*, 2021, **57**, 1392–1395.
38 E. Meggers, P. L. Holland, W. B. Tolman, F. E. Romesberg and P. G. Schultz, *J. Am. Chem. Soc.*, 2000, **122**, 10714–10715.
39 N. Zimmermann, E. Meggers and P. G. Schultz, *Bioorg. Chem.*, 2004, **32**, 13–25.
40 K. Tanaka, Y. Yamada and M. Shionoya, *J. Am. Chem. Soc.*, 2002, **124**, 8802–8803.
41 K. Tanaka, A. Tengeiji, T. Kato, N. Toyama, M. Shiro and M. Shionoya, *J. Am. Chem. Soc.*, 2002, **124**, 12494–12498.
42 Y. Takezawa, K. Tanaka, M. Yori, S. Tashiro, M. Shiro and M. Shionoya, *J. Org. Chem.*, 2008, **73**, 6092–6098.
43 C. Switzer and D. Shin, *Chem. Commun.*, 2005, **41**, 1342–1344.
44 Y. Takezawa, K. Nishiyama, T. Mashima, M. Katahira and M. Shionoya, *Chem.–Eur. J.*, 2015, **21**, 14713–14716.
45 K. Nishiyama, Y. Takezawa and M. Shionoya, *Inorg. Chim. Acta*, 2016, **452**, 176–180.
46 K. Nishiyama, K. Mori, Y. Takezawa and M. Shionoya, *Chem. Commun.*, 2021, **57**, 2487–2490.
47 Y. Takezawa, A. Suzuki, M. Nakaya, K. Nishiyama and M. Shionoya, *J. Am. Chem. Soc.*, 2020, **142**, 21640–21644.
48 D. Ukale, V. S. Shinde and T. Lönnberg, *Chem.–Eur. J.*, 2016, **22**, 7917–7923.
49 S. Johannsen, N. Megger, D. Böhme, R. K. O. Sigel and J. Müller, *Nat. Chem.*, 2010, **2**, 229–234.
50 K. Petrovec, B. J. Ravoo and J. Müller, *Chem. Commun.*, 2012, **48**, 11844–11846.
51 S. Hensel, N. Megger, K. Schweizer and J. Müller, *Beilstein J. Org. Chem.*, 2014, **10**, 2139–2144.
52 N. Sandmann, D. Defayay, A. Hepp and J. Müller, *J. Inorg. Biochem.*, 2019, **191**, 85–93.
53 K. Schweizer, J. Kösters and J. Müller, *J. Biol. Inorg Chem.*, 2015, **20**, 895–903.
54 B. A. Otter, E. A. Falco and J. J. Fox, *J. Org. Chem.*, 1969, **34**, 2636–2642.
55 C. Cadena-Amaro and S. Pochet, *Tetrahedron*, 2005, **61**, 5081–5087.
56 It has been reported that the pK_{a2} of 1-methyl-2-oxo-imidazole-4-carboxylate is greater than 13 (ref. 54). Therefore, the N3 atom of the $\mathbf{Im^{OC}}$ nucleobase is considered to be protonated under neutral conditions.
57 T. E. Spratt, *Biochemistry*, 2001, **40**, 2647–2652.
58 M. D. McCain, A. S. Meyer, S. S. Schultz, A. Glekas and T. E. Spratt, *Biochemistry*, 2005, **44**, 5647–5659.
59 E.-K. Kim and C. Switzer, *Org. Lett.*, 2014, **16**, 4059–4061.
60 S. Katz, *Biochim. Biophys. Acta*, 1963, **68**, 240–253.
61 Y. Miyake, H. Togashi, M. Tashiro, H. Yamaguchi, S. Oda, M. Kudo, Y. Tanaka, Y. Kondo, R. Sawa, T. Fujimoto, T. Machinami and A. Ono, *J. Am. Chem. Soc.*, 2006, **128**, 2172–2173.
62 A. Ono, S. Cao, H. Togashi, M. Tashiro, T. Fujimoto, T. Machinami, S. Oda, Y. Miyake, I. Okamoto and Y. Tanaka, *Chem. Commun.*, 2008, **44**, 4825–4827.
63 Y. Tanaka, S. Oda, H. Yamaguchi, Y. Kondo, C. Kojima and A. Ono, *J. Am. Chem. Soc.*, 2007, **129**, 244–245.
64 J. Kondo, T. Yamada, C. Hirose, I. Okamoto, Y. Tanaka and A. Ono, *Angew. Chem., Int. Ed.*, 2014, **53**, 2385–2388.
65 M. Flamme, C. Figazzolo, G. Gasser and M. Hollenstein, *Metallomics*, 2021, **13**, mfab016.
66 T. Kobayashi, Y. Takezawa, A. Sakamoto and M. Shionoya, *Chem. Commun.*, 2016, **52**, 3762–3765.
67 C. Kaul, M. Müller, M. Wagner, S. Schneider and T. Carell, *Nat. Chem.*, 2011, **3**, 794–800.